Conflict of interest statement

The authors confirm that there is no conflict of interest to declare.

Characterising the dynamics of placental glycogen stores in the mouse

George A.G. Roberts and Simon J. Tunster*

Centre for Trophoblast Research, Department of Physiology, Development and Neuroscience, University of Cambridge, Cambridge, CB2 3EG, UK

Running title: Placental glycogen storage in the mouse

Key words: mouse placenta, placental glycogen, glycogen cells, glucose 6-phosphatase, G6pc3

*Corresponding author email: sjt95@cam.ac.uk

Abbreviations

E	Embryonic day
FGR	Fetal growth restriction
Db	Decidua basalis
Jz	Junctional zone
Lz	Labyrinth zone
G6Pase	Glucose 6-phosphatase
GDM	Gestational diabetes mellitus
GlyT	Glycogen trophoblast
PAS	Periodic acid Schiff staining
PL1/2	Placental lactogen 1/2
PRL	Prolactin
P-TGCs	Parietal trophoblast giant cells
SpT	Spongiotrophoblast

Abstract

Introduction: The placenta performs a range of functions to support fetal growth. In addition to facilitating nutrient transport, the placenta also stores glucose as glycogen, which is thought to maintain fetal glucose supply during late gestation. However, evidence to support such a role is currently lacking. Similarly, our understanding of the dynamics of placental glycogen metabolism in normal mouse pregnancy is limited.

Methods: We quantified the placental glycogen content in wild type C57BL/6JOlaHsd mouse placentas from mid (E12.5) to late (E18.5) gestation, alongside characterising the temporal expression pattern of genes encoding glycogenesis and glycogenolysis pathway enzymes. To assess the potential of the placenta to produce glucose, we investigated the spatiotemporal expression of glucose 6-phosphatase by qPCR and *in situ* hybridisation. Separate analyses were undertaken for placentas of male and female conceptuses to account for potential sexual dimorphism.

Results: Placental glycogen stores peak at E15.5, having increased over 5-fold from E12.5, before declining by a similar extent at E18.5. Glycogen stores were 17% higher in male placentas than in females at E15.5. Expression of glycogen branching enzyme (*Gbe1*) was reduced ~40% towards term. Expression of the glucose 6-phosphatae isoform *G6pc3* was enriched in glycogen trophoblast cells and increased towards term.

Discussion: Reduced expression of *Gbe1* suggests a decline in glycogenesis, and specifically, glycogen branching towards term. Expression of *G6pc3* by glycogen trophoblasts is consistent with an ability to produce and release glucose from glycogen stores. However, the ultimate destination of the glucose generated from placental glycogen remains to be elucidated.

Highlights

- Placental glycogen stores peak at embryonic day 15.5 and decline 4-fold by E18.5
- Expression of glycogen branching enzyme *Gbe1* declines ~40% from E12.5
- The glucose 6 phosphatase isoform *G6pc3* is expressed in the mouse placenta
- *G6pc3* expression is enriched in glycogen trophoblast cells
- *G6pc3* expression in glycogen cells is consistent with glucose production

Introduction

The placenta performs a diverse range of functions to support fetal growth whilst maintaining maternal well-being. In addition to facilitating nutrient transport from mother to fetus, the placenta also stores glucose as glycogen. Aberrant placental glycogen storage is often associated with fetal growth restriction (FGR) in mouse models [1], and in humans, elevated placental glycogen has been reported in diabetic pregnancies and pre-eclampsia [2-6]. However, the normal physiological role of placental glycogen stores remains unclear [reviewed in 1, 7]. The most widely accepted hypothesis is that placental glycogen represents a readily mobilised source of glucose to support fetal growth during late gestation [8, 9]. However, direct experimental evidence for such a role is currently lacking.

The mouse is an ideal model in which to investigate the role of placental glycogen, with a short gestation, large litter size, and well-characterised placental development [10, 11]. The mature mouse placenta comprises the maternal-derived decidua basalis (Db) and the fetal-derived labyrinth and junctional zones (Lz and Jz respectively) [10, 11]. The Lz facilitates nutrient and gas exchange whereas the Jz is predominantly endocrine in function. The Jz is primarily comprised of spongiotrophoblast (SpT) and glycogen trophoblast (GlyT) cells, both of which have an endocrine role, with GlyT also responsible for glycogen storage. GlyT are first observed around embryonic day (E) 6.5, identified by the presence of small quantities of glycogen detected by periodic acid-Schiff (PAS) staining [12, 13]. Beginning around E12.5, these "pre-GlyT" transition to mature GlyT, a process seemingly driven by expression of *Gjb3* and *Cdkn1c* and marked by an increased accumulation of glycogen stores that results in the characteristic vacuolated appearance of GlyT by histology [14]. GlyT number increases nearly 300-fold between E12.5 and E16.5 before declining ~50% by E18.5 [14]. From ~E12.5, GlyT begin to invade the maternal decidua where they associate with spiral arteries that deliver maternal blood to the placenta [14-16]. The majority of GlyT cells remain within the Jz and localising around channels that drain maternal blood from the placenta [14, 16, 17].

Studies in mutant mouse models indicate that placental glycogen content declines in the days before term [18-24], consistent with a role in supporting fetal growth during late gestation [14]. However, the dynamics of placental glycogen storage and mobilization during normal gestation in the mouse have not been formally quantitated to date. Similarly, little is known about the mechanism by which placental glycogen metabolism is regulated.

In particular, expression of glucose 6-phosphatase (G6pase) by GlyT cells is essential for release of glucose that is available for fetal uptake [25]. G6pase hydrolyses the polar phosphate group of glucose 6-phosphate, the end product of glycogenolysis, to yield glucose that can be transported out of the cell. Glucose production has been demonstrated in the human placenta at term [26], with increased G6Pase activity from week 28 of gestation [27], attributable to expression of the *G6PC3* isoform [28]. However, *G6pase* expression has not been investigated in the mouse placenta to date.

The aim of this work was to characterise the dynamics of placental glycogen storage in normal mouse gestation and explore the mechanisms regulating placental glycogen metabolism. We hypothesised that determining the expression profile of *G6pase* isoforms in the mouse placenta would provide insight as to the putative function of these energy stores as a source of glucose to support fetal growth.

Materials and Methods

Animals

Animal studies and breeding were approved by the University of Cambridge Animal Welfare and Ethical Review Body in accordance with the Animals (Scientific Procedures) Act 1986. Male and female C57BL/6JOlaHsd mice were purchased from Envigo (UK) and housed throughout the study on a 12-hour light-dark cycle, receiving tap water and food (RM3(E), Special Diets Services) *ad libitum*. Females (aged 8-14 weeks) were mated with males (age 8-20 weeks), with the day of plug discovery recorded as embryonic day 0.5 (E0.5). Pregnant females were killed by cervical dislocation at the indicated gestational stages. Fetuses and placentas were separated, briefly dried on tissue paper and weighed. The yolk sac was retained for determination of fetal sex by PCR as described previously [29].

Tissue processing

Placentas were bisected, and each half weighed. Glycogen was extracted from one half of all placentas as described previously [30], and resuspended in 1 ml molecular biology grade water (Sigma). Glycogen extracts were diluted 1:4 and concentration determined using the phenol-sulphuric acid method [30]. For each litter, half of the remaining bisected placentas were fixed and processed for *in situ* hybridisation, whilst the other half were snap frozen and processed for gene expression analysis. One male and one female placenta from each

litter was used for gene expression analysis and *in situ* hybridisation. For *in situ* hybridisation, placental tissue was fixed overnight at 4°C in phosphate-buffered 4% paraformaldehyde, paraffin-embedded and 6 μm sections cut through the midline.

Quantitative and semi-quantitative gene expression analysis

Total RNA was extracted using the GenElute Mammalian Total RNA MiniPrep Kit (Sigma) with OnColumn DNase (Sigma) and 1 μg reverse transcribed in a 25 μl reaction containing 500 ng Random Primers (Promega), 0.5 mM each dNTP (ThermoFisher) and 200U M-MLV Reverse Transcriptase, RNase H minus, Point Mutant (Promega). RT reactions were diluted 15X in 10 mM Tris (pH8) and 2 μl used as template in a 10 μl qPCR reaction, comprising 0.5 μM of forward and reverse primer (Sigma); 0.2 mM each dNTP (ThermoFisher); 0.5U DreamTaq HotStart DNA Polymerase (ThermoFisher); 0.12X SybrGreen (Invitrogen) in 1X Buffer (2 mM $MgCl_2$). Reactions were run in triplicate on a DNA Engine Opticon 2 (MJ Research). Thermocycler conditions were: 94°C for 2 minutes, followed by 35 cycles of 94°C for 20 seconds, 59°C for 20 seconds and 72°C for 30 seconds, with a plate read following each cycle, and a final elongation at 72°C for 5 minutes. Melting curve analysis was performed between 70 and 90°C in 0.5°C increments, with a 2 second hold at each temperature. Cycle threshold values were determined and relative expression calculated according to the $2^{-\Delta\Delta CT}$ method [31, 32], normalising to the geometric mean of the reference genes *Polr2a* and *Ubc* [33]. Primer sequences and properties are provided in Supplementary Table 1. Semi-quantitative expression screening was conducted as described above, but omitting SybrGreen from the reaction mix, with reactions run on a MyCycler Thermocycler (BioRad) under the same conditions as above, but omitting the plate read and melting curve steps. PCR reactions were run on a 1% agarose gel and visualised with a UV transilluminator (BioRad). Primer sequences and properties are provided in Supplementary Table 2.

In situ hybridisation

The *Tpbpa* and *Prl8a8* riboprobes have been described previously [34, 35]. The *G6pc3* probe was generated by amplification of a 531-bp fragment from pooled E12.5-E18.5 placental cDNA using the primers 5'-TTTTCAGTTCTGCTTCCCCG-3' and 5'-CAATACATGAGGCTGGCACC-3', which was subsequently cloned in to the pDrive vector (Qiagen). Plasmids were

linearised and run-off DIG-labelled sense and antisense probes transcribed using the DIG RNA Labelling mix (Sigma). *In situ* hybridisation was performed on 6 μm paraffin sections as described previously [36], incorporating modifications [37], with probe hybridisation at 60^{o}C overnight.

Statistical analyses

Separate analyses were undertaken for placentas of male and female conceptuses to account for potential sexual dimorphism in glycogen storage [38]. Statistical analyses were performed by Two-Way ANOVA to identify main effects (gestational stage (P_{Stage}) and sex (P_{Sex}) and an interaction between these factors (P_{Int}). Where an effect of gestational stage was indicated, the Dunnett's test was used to perform separate planned comparisons for males and females, using E12.5 as the control stage. Where an effect of sex was identified, a two-tailed independent samples t-test was utilised to perform a planned comparison between males and females at each timepoint. Numerical data and summary statistics are provided in Supplementary Tables 3-9.

Results

Dynamics of fetal and placental growth

Fetal weight increased ~14-fold between E12.5 and E18.5, with no difference observed between sex at any stage (Fig 1A). Placental weight increased ~50% from E12.5 to E15.5 before declining slightly towards term (Fig 1B). Placental weight of female conceptuses was typically lower than that of males, achieving statistical significance at E15.5, E16.5 and E18.5 (Fig 1B). The F:P ratio increased ~10-fold between E12.5 and E18.5, with no difference between sex observed (Fig 1C). Fetal and placental weights exhibited statistically significant positive correlation at E12.5, E14.5, E15.5 and E17.5 for males, but only at E17.5 and E18.5 for females (Supp Fig 1).

Dynamics of placental glycogen storage

Total placental glycogen content increased ~5.5-fold between E12.5 and E15.5 before declining by a similar magnitude by E18.5 (Fig 1D). A similar trend was also observed when glycogen content was adjusted by placental weight (mg/g of placenta), showing that changes in glycogen content are not driven by changes in placental weight (Fig 1E). Whilst

177 total glycogen content of male placentas was 17% greater than that of females at E15.5 (Fig
178 1D), no other sex differences were observed. At its peak, placental glycogen represented
179 ~1.5% of placental weight, increasing from ~0.5% at E12.5 and declining to ~0.4% at E18.5
180 (Fig 1F). Positive correlation between fetal weight and placental glycogen was statistically
181 significant at E12.5, E14.5 and E17.5 for males and at E14.5, E16.5 and E18.5 for females (Fig
182 2). Fetal weight and placental glycogen concentration exhibited statistically significant
183 positive correlation only at E14.5 in males and at E14.5 and E16.5 in females (Supp Fig 2).
184 Heavier placentas were consistently associated with greater total glycogen content (Supp
185 Fig 3), but there was no correlation between placental weight and glycogen concentration
186 (Supp Fig 4).
187
188 *Temporal expression of trophoblast lineage markers*
189 The volume of the Jz increases ~2.5-fold from E12.5 to E16.5 [39], which may be largely
190 attributed to a ~200-fold increase in GlyT number within the Jz, with only a ~3.5-fold
191 increase in SpT number [14]. Expression of the pan-Jz markers *Tpbpa* and *Tpbpb* increased
192 from E12.5 to ~E15.5 before declining towards term (Fig 3A, B). Expression of *Pcdh12*, which
193 is specific to GlyT from ~E7.5 [13], increased ~1.5 fold between E12.5 and E15.5, before
194 declining towards term, although achieving significance only for males (Fig 3C). Expression
195 of *Gjb3*, which is specific to GlyT from ~E13.5 and coincides with the transition from pre-
196 GlyT to mature GlyT, remained relatively unchanged throughout gestation (Fig3D).
197 Expression of *Aldh1a3*, which is specific to GlyT from ~E8.5 [40], increased ~2-fold between
198 E12.5 and E15.5 before declining towards term, with expression higher in male placentas
199 until E15.5 (Fig 3E). Expression of *Prl6a1*, a marker of "non-migratory" GlyT [36], decreased
200 ~20-fold (Fig 3F), whereas expression of *Prl7b1*, a marker of "migratory" GlyT [36], was
201 relatively unchanged (Fig 3G). In contrast, expression of the SpT markers *Prl8a8* and *Prl3a1*
202 increased ~12-fold and ~800-fold respectively (Fig 3H, I). For comparison, expression of
203 lineage markers of the Lz, which increases in volume by ~4-fold between E12.5 and E18.5
204 [39], are presented in Supp Fig 5.
205
206 *Temporal expression of glycogenesis and glycogenolysis pathway genes*
207 A number of transcriptional regulators have been implicated in regulating GlyT development
208 and/or function [1]. We hypothesised that the transition from a predominantly glycogenic

state to a glycogenolytic state during late gestation is driven by a down-regulation of genes encoding glycogenesis pathway enzymes (Fig 4) and a coincident upregulation of genes encoding glycogenolysis pathway enzymes (Fig 5). Consistent with this, expression of *Gbe1*, which encodes glycogen branching enzyme, declined ~40% from E12.5 to E15.5, thereafter remaining relatively constant to term (Fig 4G). We also observed a modest decline in expression of glycogen synthase isoform *Gys1*, although this achieved statistical significance only in females (Fig 4F). Whilst two isoforms of glycogen synthase exist (*Gys1* and *Gys2*), we were unable to detect expression of the *Gys2* isoform in the mouse placenta (Supp Fig 7). Expression of the muscle isoform of glycogen phosphorylase (*Pygm*), which catalyses the rate limiting step of glycogenolysis by releasing terminal glucose subunits from glycogen branches increased ~2-fold towards term (Fig 5D).

Spatiotemporal expression of glucose 6 phosphatase

Glucose 6-phosphatase expression in GlyT is essential if their glycogen stores are to provide a source of glucose that maintains fetal nutrient supply during late gestation as suggested [14]. Whilst placental expression of the *G6pc* and *G6pc2* isoforms was not detected at any stage, we observed robust expression of *G6pc3* from E12.5 until E18.5 (Supp Fig 8). Furthermore, expression of *G6pc3* increased ~50% towards term, with expression in male placentas marginally higher than in female placentas at E17.5 (Fig 5F). As revealed by *in situ* hybridisation, *G6pc3* expression was enriched in clusters of cells located within both the Jz (black arrow heads) and Db (white arrow heads) at E15.5 (Fig 6A, D). The morphological appearance, expression of the Jz marker *Tpbpa* (Fig 6B, E) and absence of the SpT marker *Prl8a8* (Fig 6C, F), confirmed these as GlyT cells. Expression of *G6pc3* was also observed in parietal trophoblast giant cells (P-TGC) (Fig 6D; asterisks), with low expression detected in some SpT and cells of the Lz (Fig 6D, G). Hybridisation with a *G6pc3* sense probe did not yield any signal (Fig 6I).

Discussion

Dynamics of mouse placental glycogen storage

Further to previous studies indicating a broad decline in placental glycogen content towards term, here we demonstrate that placental glycogen content peaks at E15.5, having increased by over 5-fold from E12.5, before declining by a similar magnitude at E18.5. At its

maximum, placental glycogen represents ~1.5% of organ weight. This is comparable to the glycogen content of mouse liver (2-4% of organ weight) and substantially greater than in mouse skeletal muscle (~0.2% of organ weight) [41-43]. Whilst we observed modest correlation between placental glycogen content and fetal weight, this was not consistent throughout gestation or between sexes. This may be because placental glycogen is only one of many factors that ultimately determine fetal weight. Furthermore, since glucose is released into maternal blood, it will be available for uptake by all conceptuses of a litter, and as such correlation between individual fetal weights and placental glycogen content would not be expected.

Expression of Jz lineage markers

Despite the dramatic expansion in GlyT number [14], expression of the GlyT markers *Pcdh12*, *Gjb3* and *Aldh1a3* was increased only modestly. This suggests that the temporal expression of GlyT marker genes does not directly correlate with temporal changes in GlyT abundance. This may be explained if marker gene expression declines at the cellular level towards term. Consistent with this interpretation, analysis of *Gjb3* expression by Northern blot indicated only a ~2-fold increase in expression at E17.5 relative to E10.5 [44]. Similarly, PCDH12 protein abundance did not appear overtly different between E12.5 and E17.5 [13]. However, more sophisticated methods will be required to explore expression of GlyT markers at the cellular level.

Conversely, whilst the SpT population increases only ~4-fold between E12.5 and E16.5, expression of the SpT-specific markers *Prl8a8* and *Prl3a1* increased ~15-fold and ~800-fold respectively. Such upregulation of *Prl* gene expression may be integral to facilitating the increased translation of placental hormones towards term. The functions of most non-classical members of the PRL family, and the receptors through which they act, remain unknown [45, 46]. However, recent studies have suggested a role for SpT-derived signals in modulating placental glycogen metabolism [19, 47, 48]. By analysing the temporal expression pattern of *Prl* family members, we identified that expression of *Prl3c1*, *Prl7a2* and *Prl8a1*, closely parallels the dynamics of placental glycogen storage (Supp Fig 9), potentially identifying key candidates. Whilst all three genes are strongly expressed by the SpT lineage [36], conditional knockouts will be required to test their effect on placental glycogen metabolism.

Regulation of placental glycogen metabolism

We hypothesised that the temporal dynamics of placental glycogen stores would be driven by altered transcription of genes encoding enzymes involved in glycogen metabolism. Consistent with this we found that expression of *Gbe1* was downregulated ~40%, with a slight reduction in expression of *Gys1* in females. This is consistent with findings in the spiny mouse, in which placental expression of *Gbe1* and *Gys1* was also down-regulated towards term [38], suggesting a conserved mechanism regulating placental glycogen breakdown. Taken together, these data suggest that a reduction in the extent of glycogen branching, alongside upregulation of the muscle isoform of glycogen phosphorylase underlies the depletion of placental glycogen stores towards term.

Expression of glucose 6-phosphatase in the mouse placenta

Glucose 6-phosphatase activity is essential for a cell to produce glucose for uptake by other cells, tissues or organs [49]. G6pase activity has been demonstrated in the human placenta [27] attributable to expression of the *G6PC3* isoform [28]. In the mouse, expression of *G6pc3* in skeletal muscle has been suggested to contribute to blood glucose homeostasis [50]. Here we demonstrate that *G6pc3* expression in the mouse placenta is enriched in GlyT cells and increases ~50% by E18.5, coincident with the depletion of placental glycogen stores (Fig 1) and a ~50% reduction in GlyT number [14]. Placental expression of *G6pase* is consistent with a role for placental glycogen in providing a source of glucose to support fetal growth during late gestation. However, the ultimate destination of this glucose is not clear. The localisation of GlyT surrounding maternal arteries implies the potential for glucose to be released into maternal blood entering the placenta delivering nutrients for fetal uptake. Based on these cells accounting for ~30% of the total GlyT population [14] and an average litter size of 7, estimates of the glucose produced between E15.5 and E18.5 could contribute about 1-2% of the fetal requirement in late gestation [51]. The majority of GlyT surround channels that traverse the Jz draining maternal blood from the placenta, suggesting that glucose may be released into maternal blood leaving the placenta, and thus first be available for the mother. Based on these cells accounting for ~70% of the total GlyT population [14], estimates of the glucose produced between E15.5 and E18.5 could only account for <0.2% of the rate of maternal glucose utilisation during late pregnancy [51].

These calculations suggest that placental glycogen stores represent a somewhat inconsequential contribution to maternal and/or fetal glucose requirements. It is possible that placental glycogen stores are in a constant state of flux throughout gestation to ensure a constant supply of glucose to the fetus is maintained, and thus these calculations will underestimate the contribution of placental glycogen stores to maternal and/or fetal glucose requirements. Alternatively, as others have suggested [52], placental glycogen stores may instead provide energy store for the placenta itself.

No evidence for sexual dimorphism in placental glycogen metabolism

Whilst placental weight was typically lower in females and male placentas had 17% more glycogen than female placentas at E15.5, we did not observe any persistent differences in placental gene expression between placentas of male and female fetuses. However, with growing evidence that environmental and/or genetic perturbations may have sexually dimorphic effects, it is prudent to account for fetal sex in all phenotypic assessments in the context of genetic and/or environmental manipulation.

Limitations

A limitation of this study is that gene expression was assessed in whole-placental RNA extracts rather than separated placental regions. Whilst it is possible to generate Jz- and Lz-enriched samples at some gestational stages, this is not possible earlier in gestation. A second limitation is that gene expression was assessed only at the mRNA level, and thus a role for post-translational modifications cannot currently be excluded. For instance, glycogen synthase (GYS1) and glycogen synthase kinase (GSK3) are both regulated by phosphorylation [53]. Nonetheless, our approach was designed to investigate the hypothesis that the temporal dynamics of placental glycogen content is driven by changes in transcriptional activity of glycogenesis and glycogenolysis pathway genes.

Conclusions and future directions

We have demonstrated that mouse placental glycogen stores peak at E15.5, thereafter declining towards term, coincident with a steady increase in *G6pc3* expression. Whilst placental *G6pase* expression suggests the potential to produce glucose, it is beyond the

scope of this work to elucidate the ultimate destination of placenta-derived glucose. Future work will focus on addressing this question.

Acknowledgements

SJT was funded by a Next Generation Fellowship from the Centre for Trophoblast Research. We are grateful to Abby Fowden and Graham Burton for helpful discussions and to Abby Fowden for critical reading of the manuscript.

Author Contributions

SJT conceived and designed the study. GAGR and SJT performed experiments. SJT wrote the manuscript. GAGR and SJT edited and approved the final version of the manuscript.

References

[1] S. Tunster, E. Watson, A. Fowden, G.J. Burton, Placental glycogen stores and fetal growth: insights from genetic mouse models, Reproduction (2020).
[2] F. Heijkenskjold, C.A. Gemzell, Glycogen content in the placenta in diabetic mothers, Acta Paediatr 46(1) (1957) 74-80.
[3] Y.Z. Diamant, B.E. Metzger, N. Freinkel, E. Shafrir, Placental lipid and glycogen content in human and experimental diabetes mellitus, American journal of obstetrics and gynecology 144(1) (1982) 5-11.
[4] S.G. Gabbe, L.M. Demers, R.O. Greep, C.A. Villee, Placental glycogen metabolism in diabetes mellitus, Diabetes 21(12) (1972) 1185-91.
[5] G. Desoye, H.H. Hofmann, P.A. Weiss, Insulin binding to trophoblast plasma membranes and placental glycogen content in well-controlled gestational diabetic women treated with diet or insulin, in well-controlled overt diabetic patients and in healthy control subjects, Diabetologia 35(1) (1992) 45-55.
[6] V. Gheorman, L. Gheorman, C. Ivanus, R.C. Pana, A.M. Goganau, A. Patrascu, Comparative study of placenta acute fetal distress and diabetes associated with pregnancy, Rom J Morphol Embryol 54(3) (2013) 505-11.
[7] L.K. Akison, M.D. Nitert, V.L. Clifton, K.M. Moritz, D.G. Simmons, Review: Alterations in placental glycogen deposition in complicated pregnancies: Current preclinical and clinical evidence, Placenta 54 (2017) 52-58.
[8] P.M. Coan, G.J. Burton, A.C. Ferguson-Smith, Imprinted genes in the placenta--a review, Placenta 26 Suppl A (2005) S10-20.
[9] V. Barash, E. Shafrir, Mobilization of placental glycogen in diabetic rats, Placenta 11(6) (1990) 515-21.
[10] J. Rossant, J.C. Cross, Placental development: lessons from mouse mutants, Nat Rev Genet 2(7) (2001) 538-48.
[11] E.D. Watson, J.C. Cross, Development of structures and transport functions in the mouse placenta, Physiology (Bethesda) 20 (2005) 180-93.

[12] R.B. Tesser, P.L. Scherholz, L. do Nascimento, S.G. Katz, Trophoblast glycogen cells differentiate early in the mouse ectoplacental cone: putative role during placentation, Histochem Cell Biol 134(1) (2010) 83-92.
[13] S. Bouillot, C. Rampon, E. Tillet, P. Huber, Tracing the Glycogen Cells with Protocadherin 12 During Mouse Placenta Development, Placenta (2005).
[14] P.M. Coan, N. Conroy, G.J. Burton, A.C. Ferguson-Smith, Origin and characteristics of glycogen cells in the developing murine placenta, Dev Dyn 235(12) (2006) 3280-94.
[15] R.W. Redline, C.L. Chernicky, H.Q. Tan, J. Ilan, J. Ilan, Differential expression of insulin-like growth factor-II in specific regions of the late (post day 9.5) murine placenta, Mol Reprod Dev 36(2) (1993) 121-9.
[16] M. Gasperowicz, C. Surmann-Schmitt, Y. Hamada, F. Otto, J.C. Cross, The transcriptional co-repressor TLE3 regulates development of trophoblast giant cells lining maternal blood spaces in the mouse placenta, Dev Biol 382(1) (2013) 1-14.
[17] P.M. Coan, A.C. Ferguson-Smith, G.J. Burton, Ultrastructural changes in the interhaemal membrane and junctional zone of the murine chorioallantoic placenta across gestation, J Anat 207(6) (2005) 783-96.
[18] M.F. Lopez, P. Dikkes, D. Zurakowski, L. Villa-Komaroff, Insulin-like growth factor II affects the appearance and glycogen content of glycogen cells in the murine placenta, Endocrinology 137(5) (1996) 2100-8.
[19] S.J. Tunster, B. Tycko, R.M. John, The imprinted Phlda2 gene regulates extraembryonic energy stores, Mol Cell Biol 30(1) (2010) 295-306.
[20] C. Duval, M.R. Dilworth, S.J. Tunster, S.J. Kimber, J.D. Glazier, PTHrP is essential for normal morphogenetic and functional development of the murine placenta, Dev Biol 430(2) (2017) 325-336.
[21] A.N. Sferruzzi-Perri, O.R. Vaughan, M. Haro, W.N. Cooper, B. Musial, M. Charalambous, D. Pestana, S. Ayyar, A.C. Ferguson-Smith, G.J. Burton, M. Constancia, A.L. Fowden, An obesogenic diet during mouse pregnancy modifies maternal nutrient partitioning and the fetal growth trajectory, FASEB J 27(10) (2013) 3928-37.
[22] S.J. Tunster, G.I. McNamara, H.D. Creeth, R.M. John, Increased dosage of the imprinted Ascl2 gene restrains two key endocrine lineages of the mouse Placenta, Dev Biol 418(1) (2016) 55-65.
[23] S.J. Tunster, M. Van De Pette, R.M. John, Isolating the role of elevated Phlda2 in asymmetric late fetal growth restriction in mice, Dis Model Mech 7(10) (2014) 1185-91.
[24] S.J. Tunster, M. Van de Pette, R.M. John, Fetal overgrowth in the Cdkn1c mouse model of Beckwith-Wiedemann syndrome, Dis Model Mech 4(6) (2011) 814-21.
[25] A.D. Chiquoine, Further studies on the histochemistry of glucose-6-phosphatase, J Histochem Cytochem 3(6) (1955) 471-8.
[26] C.H. Prendergast, K.H. Parker, R. Gray, S. Venkatesan, P. Bannister, J. Castro-Soares, K.W. Murphy, R.W. Beard, L. Regan, S. Robinson, P. Steer, D. Halliday, D.G. Johnston, Glucose production by the human placenta in vivo, Placenta 20(7) (1999) 591-8.
[27] S. Matsubara, T. Takizawa, I. Sato, Glucose-6-phosphatase is present in normal and pre-eclamptic placental trophoblasts: ultrastructural enzyme-histochemical evidence, Placenta 20(1) (1999) 81-5.
[28] O. Guionie, E. Clottes, K. Stafford, A. Burchell, Identification and characterisation of a new human glucose-6-phosphatase isoform, FEBS Lett 551(1-3) (2003) 159-64.
[29] S.J. Tunster, Genetic sex determination of mice by simplex PCR, Biol Sex Differ 8(1) (2017) 31.

[30] S. Lo, J.C. Russell, A.W. Taylor, Determination of glycogen in small tissue samples, J Appl Physiol 28(2) (1970) 234-6.
[31] K.J. Livak, T.D. Schmittgen, Analysis of relative gene expression data using real-time quantitative PCR and the 2(-Delta Delta C(T)) Method, Methods 25(4) (2001) 402-8.
[32] T.D. Schmittgen, K.J. Livak, Analyzing real-time PCR data by the comparative C(T) method, Nat Protoc 3(6) (2008) 1101-8.
[33] M.E. Solano, K. Thiele, M.K. Kowal, P.C. Arck, Identification of suitable reference genes in the mouse placenta, Placenta 39 (2016) 7-15.
[34] K.R. Lescisin, S. Varmuza, J. Rossant, Isolation and characterization of a novel trophoblast-specific cDNA in the mouse, Genes Dev 2(12A) (1988) 1639-46.
[35] S.J. Tunster, M. Van De Pette, R.M. John, Impact of genetic background on placental glycogen storage in mice, Placenta 33(2) (2012) 124-7.
[36] D.G. Simmons, S. Rawn, A. Davies, M. Hughes, J.C. Cross, Spatial and temporal expression of the 23 murine Prolactin/Placental Lactogen-related genes is not associated with their position in the locus, BMC Genomics 9 (2008) 352.
[37] J. Rakoczy, N. Padmanabhan, A.M. Krzak, J. Kieckbusch, T. Cindrova-Davies, E.D. Watson, Dynamic expression of TET1, TET2, and TET3 dioxygenases in mouse and human placentas throughout gestation, Placenta 59 (2017) 46-56.
[38] B.A. O'Connell, K.M. Moritz, D.W. Walker, H. Dickinson, Treatment of pregnant spiny mice at mid gestation with a synthetic glucocorticoid has sex-dependent effects on placental glycogen stores, Placenta 34(10) (2013) 932-40.
[39] P.M. Coan, A.C. Ferguson-Smith, G.J. Burton, Developmental dynamics of the definitive mouse placenta assessed by stereology, Biol Reprod 70(6) (2004) 1806-13.
[40] J.E. Outhwaite, B.V. Natale, D.R. Natale, D.G. Simmons, Expression of aldehyde dehydrogenase family 1, member A3 in glycogen trophoblast cells of the murine placenta, Placenta 36(3) (2015) 304-11.
[41] G. Testoni, J. Duran, M. Garcia-Rocha, F. Vilaplana, A.L. Serrano, D. Sebastian, I. Lopez-Soldado, M.A. Sullivan, F. Slebe, M. Vilaseca, P. Munoz-Canoves, J.J. Guinovart, Lack of Glycogenin Causes Glycogen Accumulation and Muscle Function Impairment, Cell Metab 26(1) (2017) 256-266 e4.
[42] M. Sakaida, J. Watanabe, S. Kanamura, H. Tokunaga, R. Ogawa, Physiological role of skeletal muscle glycogen in starved mice, Anat Rec 218(3) (1987) 267-74.
[43] Y. Lee, E.D. Berglund, M.Y. Wang, X. Fu, X. Yu, M.J. Charron, S.C. Burgess, R.H. Unger, Metabolic manifestations of insulin deficiency do not occur without glucagon action, Proc Natl Acad Sci U S A 109(37) (2012) 14972-6.
[44] A. Plum, E. Winterhager, J. Pesch, J. Lautermann, G. Hallas, B. Rosentreter, O. Traub, C. Herberhold, K. Willecke, Connexin31-deficiency in mice causes transient placental dysmorphogenesis but does not impair hearing and skin differentiation, Dev Biol 231(2) (2001) 334-47.
[45] M.J. Soares, S.M.K. Alam, T. Konno, J.K. Ho-Chen, R. Ain, The prolactin family and pregnancy-dependent adaptations, Anim Sci J 77(1) (2006) 1-9.
[46] M.J. Soares, T. Konno, S.M. Alam, The prolactin family: effectors of pregnancy-dependent adaptations, Trends Endocrinol Metab 18(3) (2007) 114-21.
[47] S.J. Tunster, H.D. Creeth, R.M. John, The imprinted Phlda2 gene modulates a major endocrine compartment of the placenta to regulate placental demands for maternal resources, Dev Biol (2015).

[48] D.J. Pennisi, G. Kinna, H.S. Chiu, D.G. Simmons, L. Wilkinson, M.H. Little, Crim1 has an essential role in glycogen trophoblast cell and sinusoidal-trophoblast giant cell development in the placenta, Placenta 33(3) (2012) 175-82.
[49] S. Matsubara, I. Sato, Glucose production and glucose-6-phosphatase in the human placenta, Placenta 21(5-6) (2000) 591-3.
[50] J.J. Shieh, C.J. Pan, B.C. Mansfield, J.Y. Chou, A potential new role for muscle in blood glucose homeostasis, J Biol Chem 279(25) (2004) 26215-9.
[51] B. Musial, D.S. Fernandez-Twinn, O.R. Vaughan, S.E. Ozanne, P. Voshol, A.N. Sferruzzi-Perri, A.L. Fowden, Proximity to Delivery Alters Insulin Sensitivity and Glucose Metabolism in Pregnant Mice, Diabetes 65(4) (2016) 851-60.
[52] V. Barash, A. Riskin, E. Shafrir, I.D. Waddell, A. Burchell, Kinetic and immunologic evidence for the absence of glucose-6-phosphatase in early human chorionic villi and term placenta, Biochim Biophys Acta 1073(1) (1991) 161-7.
[53] E. Beurel, S.F. Grieco, R.S. Jope, Glycogen synthase kinase-3 (GSK3): regulation, actions, and diseases, Pharmacol Ther 148 (2015) 114-31.

Figure Legends

Figure 1: Dynamics of fetal and placental growth and placental glycogen storage. Fetal **(A)** and placental **(B)** weight, and F:P ratios **(C)** at the indicated gestational stages. Total placental content (mg) **(D)** and glycogen per g of placenta (mg/g) **(E)** calculated as the total placental glycogen content adjusted by placental weight. **F)** Placental glycogen expressed as a percentage of placental weight. Weight data (for A, B, C) from at least 10 litters at each time-point: E12.5 (males: n = 33; females: n = 41), E14.5 (males: n = 43; females: n = 30), E15.5 (males: n = 32; females: n = 34), E16.5 (males: n = 40; females: n = 32), E17.5 (males: n = 42; females: n = 32), E18.5 (males: n = 30; females: n = 40). Glycogen data (for D, E, F) from at least 10 litters at each time-point: E12.5 (males: n = 31; females: n = 33), E14.5 (males: n = 40; females: n = 28), E15.5 (males: n = 28; females: n = 31), E16.5 (males: n = 40; females: n = 32), E17.5 (males: n = 42; females: n = 32), E18.5 (males: n = 29; females: n = 37). All data is displayed as mean ± SEM, with males plotted as a solid line and females plotted as a dashed line. Main effects were tested by Two-Way ANOVA for gestational stage (P_{Stage}) and sex (P_{Sex}) and an interaction between factors (P_{Int}). A Dunnett's test was used to compare each gestational stage to E12.5. Statistical significance between males and females at each timepoint was performed by t-test. Statistical significance is indicated by: a – significantly different to E12.5 for males; b – significantly different to E12.5 for females; c – males and females differ significantly at the indicated stage.

Figure 2: Inconsistent correlation between fetal weight and total placental glycogen content. Scatter plots of total placental glycogen content (mg; x-axis) versus fetal weight (g; y-axis) for males **(A, C, E, G, I, K)** and females **(B, D, F, H, J, L)** at E12.5 **(A, B)**, E14.5 **(C, D)**, E15.5 **(E, F)**, E16.5 **(G, H)**, E17.5 **(I, J)**, and E18.5 **(K, L)**. Pearson's r correlation coefficient and the associated *p* value are displayed. Data from at least 10 litters at each time-point: E12.5 (males: n = 31; females: n = 33), E14.5 (males: n = 40; females: n = 28), E15.5 (males: n = 28; females: n = 31), E16.5 (males: n = 40; females: n = 32), E17.5 (males: n = 42; females: n = 32), E18.5 (males: n = 29; females: n = 37).

Figure 3: Temporal expression of key junctional zone lineage markers. Expression of established gene markers for junctional zone (Jz; *Tpbpa* **(A)**, *Tpbpb* **(B)**), glycogen trophoblast (GlyT; *Pcdh12* **(C)**, *Gjb3* **(D)**, *Aldh1a3* **(E)**, *Prl6a1* **(F)**, *Prl7b1* **(G)**) and

spongiotrophoblast (SpT; *Prl8a8* **(H)**, *Prl3a1* **(I)**) lineages was assessed by quantitative qPCR. All data is displayed as mean ± SEM, with data from males plotted as a solid line and from females as a dashed line. Main effects were tested by Two-Way ANOVA for gestational stage (P_{Stage}) and sex (P_{Sex}) and an interaction between factors (P_{Int}). A Dunnett's test was used to compare each gestational stage to E12.5. Statistical significance between males and females at each timepoint was performed by t-test. Statistical significance is indicated by: a – significantly different to E12.5 for males; b – significantly different to E12.5 for females; c – males and females differ significantly at the indicated stage. N = 10 individuals per sex, per timepoint, from 10 litters.

Figure 4: Temporal expression of genes encoding glycogenesis pathway enzymes. A) Schematic of glycogenesis pathway showing enzymes and the genes that encode them. Temporal expression glycogenesis pathway genes *Hk1* **(B)**, *Hk2* **(C)**, *Ugp2* **(D)**, *Gyg* **(E)**, *Gys1* **(F)**, *Gbe1* **(G)**, *Gsk3a* **(H)** and *Gsk3b* **(I)**. All data is displayed as mean ± SEM, with data from males plotted as a solid line and from females as a dashed line. Main effects were tested by Two-Way ANOVA for gestational stage (P_{Stage}) and sex (P_{Sex}) and an interaction between factors (P_{Int}). A Dunnett's test was used to compare each gestational stage to E12.5. Statistical significance between males and females at each timepoint was performed by t-test. Statistical significance is indicated by: a – significantly different to E12.5 for males; b – significantly different to E12.5 for females; c – males and females differ significantly at the indicated stage. N = 10 individuals per sex, per timepoint, from 10 litters.

Figure 5: Temporal expression of genes encoding glycogenolysis pathway enzymes. A) Schematic of glycogenolysis pathway showing enzymes and the genes that encode them. Expression of the glycogenolysis pathway genes *Pygb* **(B)**, *Pygl* **(C),** *Pygm* **(D)**, *Agl* **(E)**, and *G6pc3* **(F)**. All qPCR data is displayed as mean ± SEM, with data from males plotted as a solid line and from females as a dashed line. Main effects were tested by Two-Way ANOVA for gestational stage (P_{Stage}) and sex (P_{Sex}) and an interaction between factors (P_{Int}). A Dunnett's test was used to compare each gestational stage to E12.5. Statistical significance between males and females at each timepoint was performed by t-test. Statistical significance is indicated by: a – significantly different to E12.5 for males; b – significantly different to E12.5

for females; c – males and females differ significantly at the indicated stage. N = 10 individuals per sex, per timepoint, from 10 litters.

Figure 6: Spatial expression of *G6pc3* in the E15.5 placenta. *In situ* hybridisation demonstrated expression of *G6pc3* in the Jz and Decidua at E15.5 **(A)**. *G6pc3* positive cells were identified as glycogen cells based on morphology, expression of *Tpbpa* **(B)** and absence of *Prl8a8* expression **(C)**. **D)** Higher magnification of **(A)** reveals strong expression of *G6pc3* in GlyT clusters within both the Jz (black arrows) and decidua (white arrows). *G6pc3* expression was also observed in P-TGCs (asterisks). **(E)** and **(F)** Higher magnification of **(C B)** and **(C)** respectively confirms the presence of *Tpbpa* and absence of *Prl8a8* in *G6pc3*-positive clusters. Low level *G6pc3* expression was also observed in SpT and in scattered cells within the Lz **(G)**, with *Tpbpa* staining showing the Jz:Lz boundary **(H)**. No signal was detected with the *G6pc3* sense probe **(I)**. Scale bars: low magnification (A, B, C), 250 μm; high magnification (D, E, F, G, H, I), 100 μm.

Supplementary Figure 1: Contrasting correlation between fetal weight and placental weight between males and females. Scatter plots of total placental weight (mg; x-axis) versus fetal weight (g; y-axis) for males **(A, C, E, G, I, K)** and females **(B, D, F, H, J, L)** at E12.5 **(A, B)**, E14.5 **(C, D)**, E15.5 **(E, F)**, E16.5 **(G, H)**, E17.5 **(I, J)**, and E18.5 **(K, L)**. Pearson's r correlation coefficient and its associated *p* value are displayed. Data from at least 10 litters at each time-point: E12.5 (males: n = 33; females: n = 41), E14.5 (males: n = 43; females: n = 30), E15.5 (males: n = 32; females: n = 34), E16.5 (males: n = 40; females: n = 32), E17.5 (males: n = 42; females: n = 32), E18.5 (males: n = 30; females: n = 40).

Supplementary Figure 2: No correlation between fetal weight and placental glycogen concentration. Scatter plots of placental glycogen concentration (mg/g; x-axis) versus fetal weight (g; y-axis) for males (A, C, E, G, I, K) and females (B, D, F, H, J, L) at E12.5 (A, B), E14.5 (C, D), E15.5 (E, F), E16.5 (G, H), E17.5 (I, J), and E18.5 (K, L). Pearson's r correlation coefficient and its associated *p* value are displayed. Data from at least 10 litters at each time-point: E12.5 (males: n = 31; females: n = 33), E14.5 (males: n = 40; females: n = 28), E15.5 (males: n = 28; females: n = 31), E16.5 (males: n = 40; females: n = 32), E17.5 (males: n = 42; females: n = 32), E18.5 (males: n = 29; females: n = 37).

Supplementary Figure 3: Heavier placentas accumulate greater glycogen stores. Scatter plots of placental weight (mg; x-axis) versus total placental glycogen (mg; y-axis) for males (A, C, E, G, I, K) and females (B, D, F, H, J, L) at E12.5 (A, B), E14.5 (C, D), E15.5 (E, F), E16.5 (G, H), E17.5 (I, J), and E18.5 (K, L). Pearson's r correlation coefficient and its associated *p* value are displayed. Data from at least 10 litters at each time-point: E12.5 (males: n = 31; females: n = 33), E14.5 (males: n = 40; females: n = 28), E15.5 (males: n = 28; females: n = 31), E16.5 (males: n = 40; females: n = 32), E17.5 (males: n = 42; females: n = 32), E18.5 (males: n = 29; females: n = 37).

Supplementary Figure 4: No correlation between placental weight and glycogen concentration. Scatter plots of placental weight (mg; x-axis) versus placental glycogen concentration (mg/g; y-axis) for males (A, C, E, G, I, K) and females (B, D, F, H, J, L) at E12.5 (A, B), E14.5 (C, D), E15.5 (E, F), E16.5 (G, H), E17.5 (I, J), and E18.5 (K, L). Pearson's r correlation coefficient and its associated *p* value are displayed. Data from at least 10 litters at each time-point: E12.5 (males: n = 31; females: n = 33), E14.5 (males: n = 40; females: n = 28), E15.5 (males: n = 28; females: n = 31), E16.5 (males: n = 40; females: n = 32), E17.5 (males: n = 42; females: n = 32), E18.5 (males: n = 29; females: n = 37).

Supplementary Figure 5: Temporal expression of key labyrinth zone lineage markers. Expression of the pan-Lz marker *Dlx3* **(A)**, syncytiotrophoblast layer I (SynT-I) marker *Syna* **(B)**, syncytiotrophoblast layer II (SynT-II) markers *Gcm1* **(C)** and *Synb* **(D)**, fetal endothelium marker *Flk1* **(E)**, and the VEGF receptor 1 *Flt1* **(F)**. All qPCR data is displayed as mean ± SEM, with data from males plotted as a solid line and from females as a dashed line. Main effects were tested by Two-Way ANOVA for gestational stage (P_{Stage}) and sex (P_{Sex}) and an interaction between factors (P_{Int}). A Dunnett's test was used to compare each gestational stage to E12.5. Statistical significance between males and females at each timepoint was performed by t-test. Statistical significance is indicated by: a – significantly different to E12.5 for males; b – significantly different to E12.5 for females; c – males and females differ significantly at the indicated stage. N = 10 individuals per sex, per timepoint, from 10 litters.

Supplementary Figure 6: Expression of phosphoglucomutase genes. Expression of *Pgm1* **(A)**, *Pgm2* **(B)** and *Pgm3* **(C).** All qPCR data is displayed as mean ± SEM, with data from males

plotted as a solid line and from females as a dashed line. Main effects were tested by Two-Way ANOVA for gestational stage (P_{Stage}) and sex (P_{Sex}) and an interaction between factors (P_{Int}). A Dunnett's test was used to compare each gestational stage to E12.5. Statistical significance between males and females at each timepoint was performed by t-test. Statistical significance is indicated by: a – significantly different to E12.5 for males; b – significantly different to E12.5 for females; c – males and females differ significantly at the indicated stage. N = 10 individuals per sex, per timepoint, from 10 litters.

Supplementary Figure 7: *Gys1* and *Gys2* sequences are highly homologous. A) Sequence alignment of the glycogen synthase isoforms *Gys1* (top) and *Gys2* (bottom) shows high sequence homology, with homologous sequence in black and mismatches in red. The entire *Gys2* sequence is shown. The *Gys1* sequence is truncated at nucleotide 2681 for space reasons (nucleotides 2682 – 3681 not shown). Locations of previously published (yellow) and novel (blue) primers highlighted. The forward primer utilised in this work spans a 12 bp deletion in the *Gys1* sequence to ensure specificity for *Gys2*. **B)** Placental expression of *Gys1* was detected at all stages examined, but *Gys2* was not expressed at any stage **(C)**. Sample order: Lanes 1 – 6 = Pooled cDNA from E12.5, E14.5, E15.5, E16.5, E17.5, E18.5 placentas respectively. Lane 7 = positive control (pooled E18.5 fetal liver cDNA). Lane 8 = no template control (NTC).

Supplementary Figure 8: PCR expression screen of glucose 6-phosphatase isoforms. Expression of the *G6pc* and *G6pc2* glucose 6 phosphatase isoforms could not be detected in the mouse placenta, but robust expression of *G6pc3* was observed at all stages examined. Pooled cDNA from E12.5, E14.5, E15.5, E16.5, E17.5, E18.5 placentas, was used as template alongside a positive control (E18.5 fetal liver cDNA for *G6pc* and *G6pc3*; cDNA reverse transcribed from C57BL/6 mouse pancreas RNA (AMS Biotechnology MR-313-C57) for *G6pc2*). NTC = no template control.

Supplementary Figure 9: Temporal expression of *Prl* gene family members. *Prl3c1* **(A)**, *Prl7a2* **(B)**, *Prl8a1* **(C)**, *Prl3b1* **(D)**, *Prl7c1* **(E)** and *Prl8a9* **(F)** exhibited an initial increase in expression followed either by a decline (*Prl3c1*, *Prl8a1*, *Prl7a2*) or plateau (*Prl3b1*, *Prl7c1*, *Prl8a9*) towards term. Expression of *Prl8a6* **(G)**, *Prl5a1* **(H)** and *Prl2a1* **(I)** continued to

increase towards term. Expression of *Prl4a1* **(J)**, *Prl7a1* **(K)** and *Prl7d1* **(L)** decreased from E12.5 to term. We did not characterise *Prl3d*, which is expressed only in parietal TGCs until ~E10.5; *Prl8a2*, which is expressed solely in the decidua; or *Prl2c*, expression of which peaks at ~E9.5 before declining dramatically thereafter [27]. Although *Prl2a1* and *Prl7c1* are not expressed by the SpT lineage their temporal expression profiles were characterised for comparison as both genes are expressed by GlyT [27]. All qPCR data is displayed as mean ± SEM, with data from males plotted as a solid line and from females as a dashed line. Main effects were tested by Two-Way ANOVA for gestational stage (P_{Stage}) and sex (P_{Sex}) and an interaction between factors (P_{Int}). A Dunnett's test was used to compare each gestational stage to E12.5. Statistical significance between males and females at each timepoint was performed by t-test. Statistical significance is indicated by: a – significantly different to E12.5 for males; b – significantly different to E12.5 for females; c – males and females differ significantly at the indicated stage. N = 10 individuals per sex, per timepoint, from 10 litters.

Figures

Figure 1

Click here to download Figure: Figures.pptx

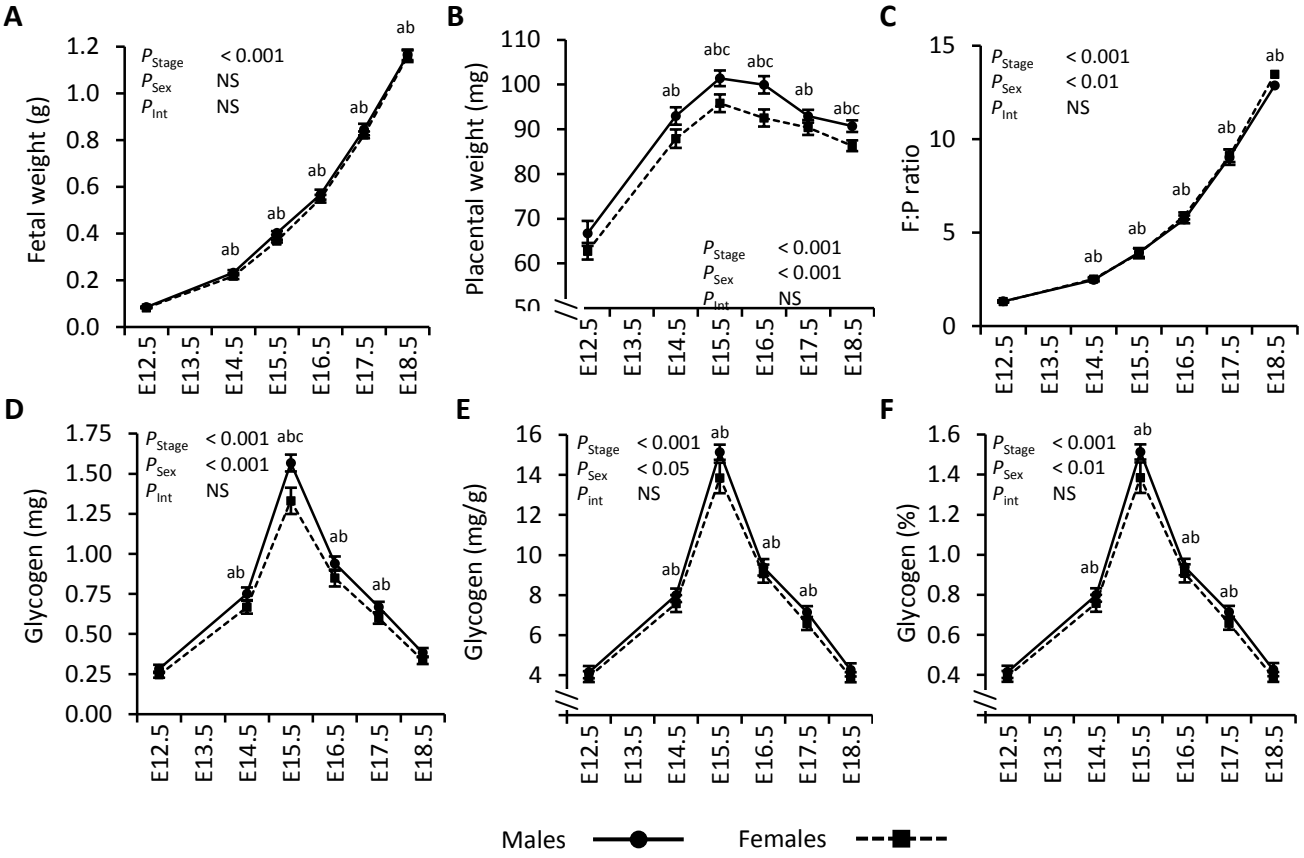

Figure 2

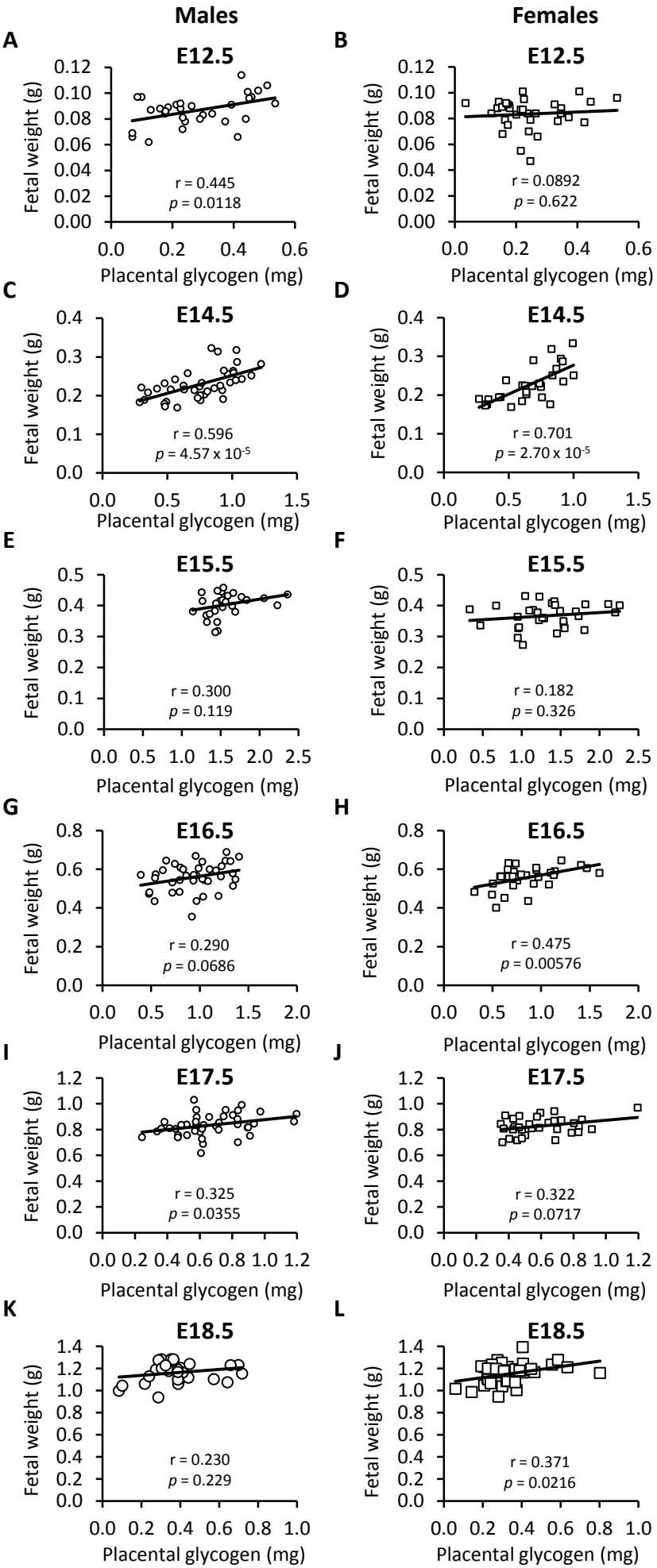
Males
Females
A
E12.5
r = 0.445
p = 0.0118
B
E12.5
r = 0.0892
p = 0.622
C
E14.5
r = 0.596
p = 4.57 x 10-5
D
E14.5
r = 0.701
p = 2.70 x 10-5
E
E15.5
r = 0.300
p = 0.119
F
E15.5
r = 0.182
p = 0.326
G
E16.5
r = 0.290
p = 0.0686
H
E16.5
r = 0.475
p = 0.00576
I
E17.5
r = 0.325
p = 0.0355
J
E17.5
r = 0.322
p = 0.0717
K
E18.5
r = 0.230
p = 0.229
L
E18.5
r = 0.371
p = 0.0216
Fetal weight (g)
Placental glycogen (mg)

Figure 3

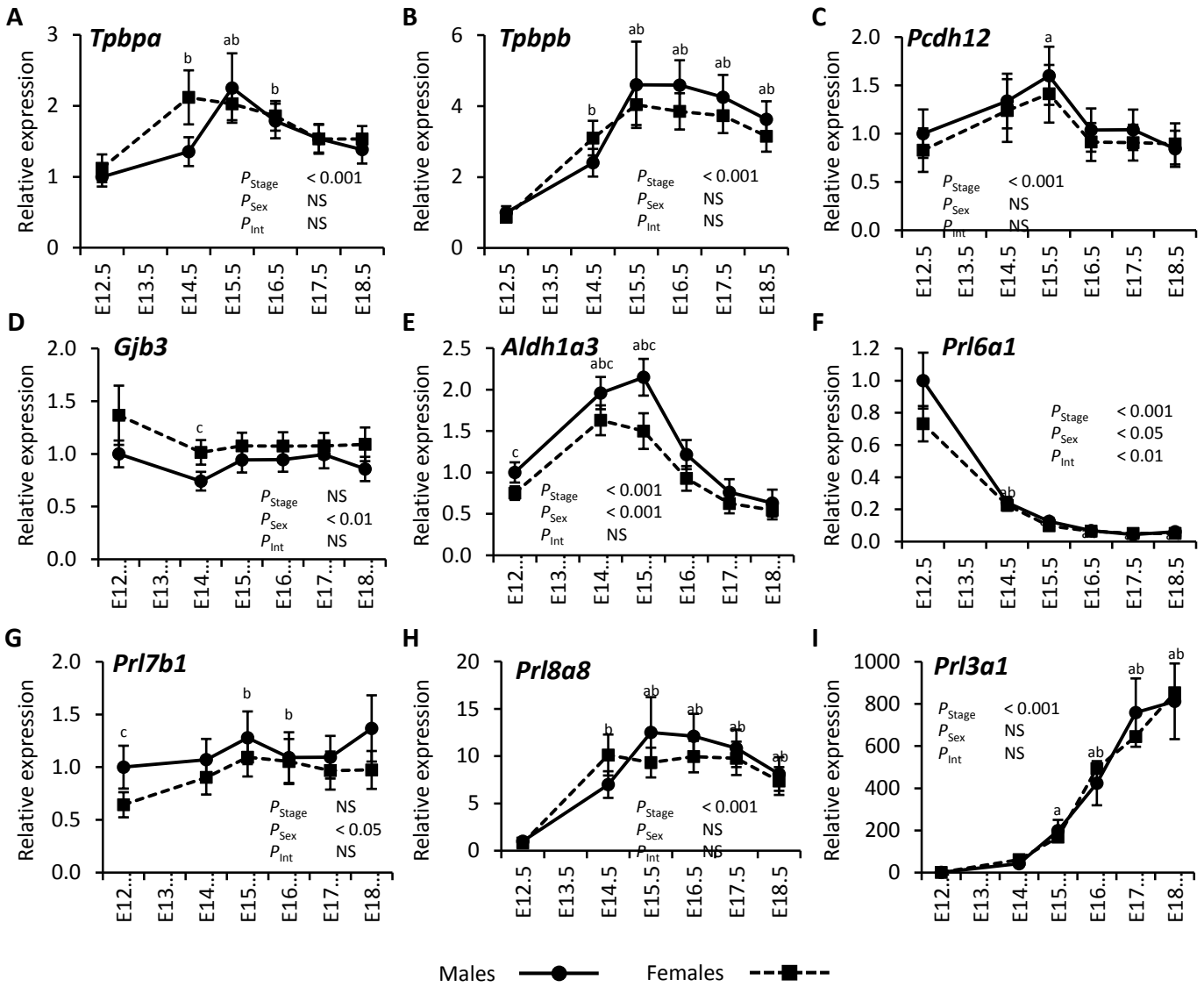
A
Tpbpa
Relative expression
b
ab
b
P_{Stage} < 0.001
P_{Sex} NS
P_{Int} NS
B
Tpbpb
b
ab
ab
ab
ab
P_{Stage} < 0.001
P_{Sex} NS
P_{Int} NS
C
Pcdh12
a
P_{Stage} < 0.001
P_{Sex} NS
P_{Int} NS
D
Gjb3
c
P_{Stage} NS
P_{Sex} < 0.01
P_{Int} NS
E
Aldh1a3
c
abc
abc
P_{Stage} < 0.001
P_{Sex} < 0.001
P_{Int} NS
F
Prl6a1
ab
P_{Stage} < 0.001
P_{Sex} < 0.05
P_{Int} < 0.01
G
Prl7b1
c
b
b
P_{Stage} NS
P_{Sex} < 0.05
P_{Int} NS
H
Prl8a8
b
ab
ab
ab
ab
P_{Stage} < 0.001
P_{Sex} NS
P_{Int} NS
I
Prl3a1
a
ab
ab
ab
P_{Stage} < 0.001
P_{Sex} NS
P_{Int} NS
E12.5
E13.5
E14.5
E15.5
E16.5
E17.5
E18.5
Males
Females

Figure 4

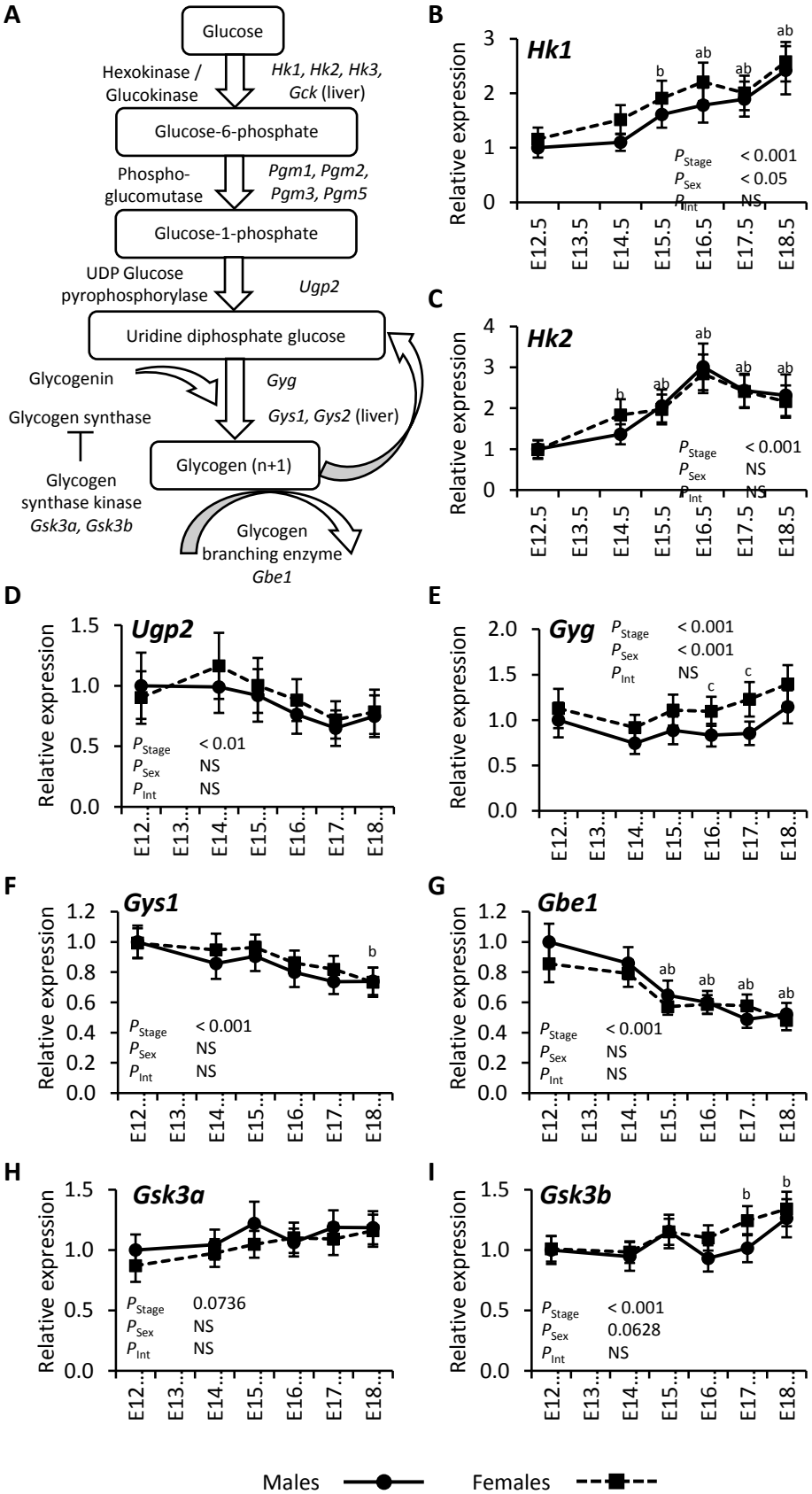
A
Glucose
Hexokinase / Glucokinase
Hk1, Hk2, Hk3, Gck (liver)
Glucose-6-phosphate
Phospho-glucomutase
Pgm1, Pgm2, Pgm3, Pgm5
Glucose-1-phosphate
UDP Glucose pyrophosphorylase
Ugp2
Uridine diphosphate glucose
Glycogenin
Gyg
Glycogen synthase
Gys1, Gys2 (liver)
Glycogen (n+1)
Glycogen synthase kinase Gsk3a, Gsk3b
Glycogen branching enzyme Gbe1
B
Hk1
Relative expression
P Stage < 0.001
P Sex < 0.05
P Int NS
C
Hk2
Relative expression
P Stage < 0.001
P Sex NS
P Int NS
D
Ugp2
Relative expression
P Stage < 0.01
P Sex NS
P Int NS
E
Gyg
Relative expression
P Stage < 0.001
P Sex < 0.001
P Int NS
F
Gys1
Relative expression
P Stage < 0.001
P Sex NS
P Int NS
G
Gbe1
Relative expression
P Stage < 0.001
P Sex NS
P Int NS
H
Gsk3a
Relative expression
P Stage 0.0736
P Sex NS
P Int NS
I
Gsk3b
Relative expression
P Stage < 0.001
P Sex 0.0628
P Int NS
E12.5
E13.5
E14.5
E15.5
E16.5
E17.5
E18.5
Males
Females

Figure 5

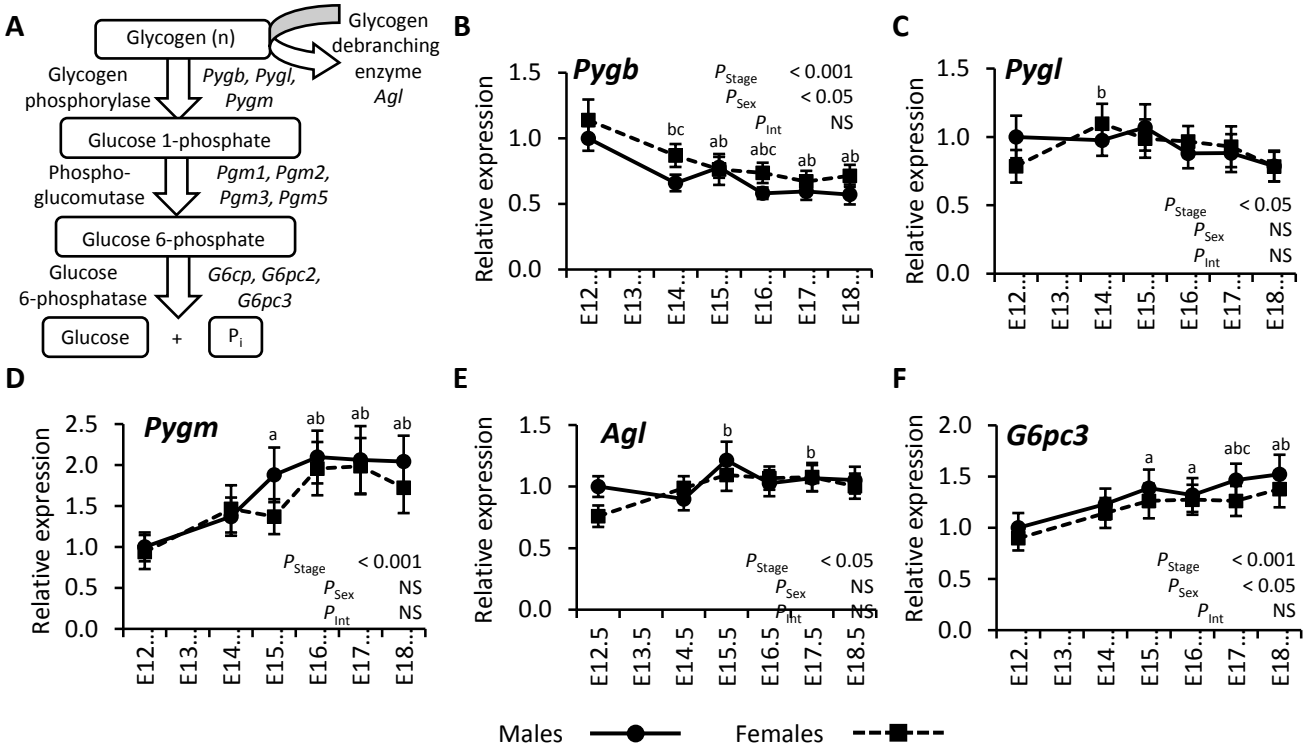
A
Glycogen (n)
Glycogen debranching enzyme Agl
Glycogen phosphorylase
Pygb, Pygl, Pygm
Glucose 1-phosphate
Phospho-glucomutase
Pgm1, Pgm2, Pgm3, Pgm5
Glucose 6-phosphate
Glucose 6-phosphatase
G6cp, G6pc2, G6pc3
Glucose
+
P_i
B
Pygb
P_Stage < 0.001
P_Sex < 0.05
P_Int NS
Relative expression
C
Pygl
P_Stage < 0.05
P_Sex NS
P_Int NS
D
Pygm
P_Stage < 0.001
P_Sex NS
P_Int NS
E
Agl
P_Stage < 0.05
P_Sex NS
P_Int NS
F
G6pc3
P_Stage < 0.001
P_Sex < 0.05
P_Int NS
E12...
E13...
E14...
E15...
E16...
E17...
E18...
E12.5
E13.5
E14.5
E15.5
E16.5
E17.5
E18.5
Males
Females

Figure 6

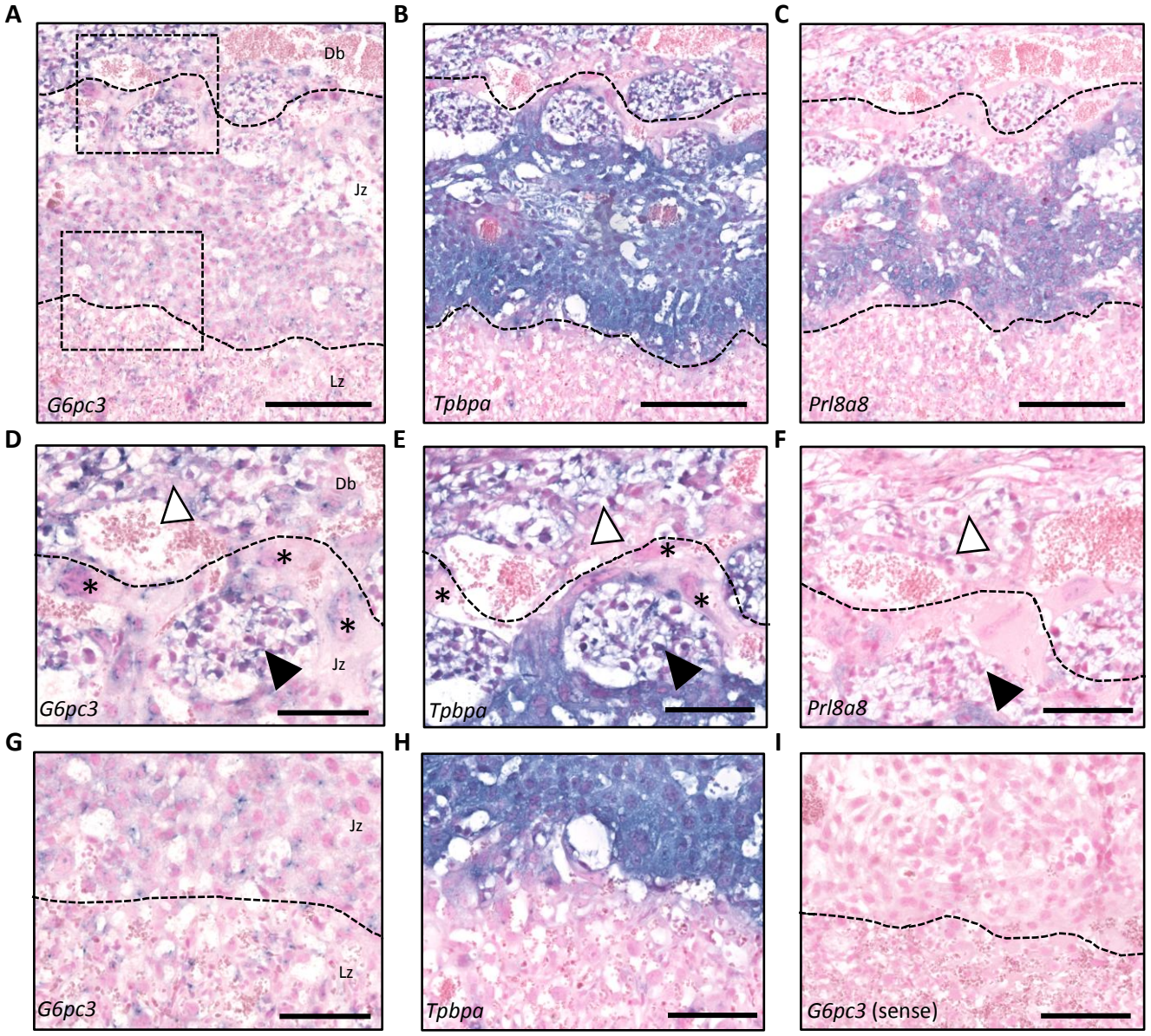
A
Db
Jz
Lz
G6pc3
B
Tpbpa
C
Prl8a8
D
Db
Jz
G6pc3
E
Tpbpa
F
Prl8a8
G
Jz
Lz
G6pc3
H
Tpbpa
I
G6pc3 (sense)

Supplementary Figures

Click here to download Supplementary File: Supplementary Figures.pptx

Supplementary Tables

Click here to download Supplementary File: Supplementary Tables.docx